Ordering and orientational glass transition of (cyanoadamantane)$_{1-x}$ (chloroadamantane)$_x$ mixed compounds

1992 J. Phys.: Condens. Matter 4 9509

(http://iopscience.iop.org/0953-8984/4/48/006)

J. Phys.: Condens. Matter 4 (1992) 9509–9516. Printed in the UK

Ordering and orientational glass transition of (cyanoadamantane)$_{1-x}$ (chloroadamantane)$_x$ mixed compounds

J F Willart†, M Descamps†, M Bertault‡ and N Benzakour†

† Laboratoire de Dynamique et Structure des Matériaux Moléculaires, Unité de Recherche associée au CNRS 801, Université de Lille 1, Bâtiment P5, F 59655 Villeneuve d'Ascq, France

‡ Groupe Matière Condensée et Matériaux, Unité de Recherche associée au CNRS 804, Université de Rennes 1, 35042 Rennes, France

Received 20 July 1992

Abstract. Equilibrium and glass properties of (cyanoadamantane)$_{1-x}$ (chloroadamantane)$_x$ mixed compounds for $x = 0.25$ have been investigated by powder and single-crystal x-ray diffraction and by differential scanning calorimetry. This plastic crystal shares with cyanoadamantane the property of forming a glassy crystal but it appears to be a better glass former. From the jump in C_p at the glass transition it can be classified as between fragile and strong glassy crystals.

1. Introduction

When crystalline phases showing an orientational disorder of the molecules are supercooled, they appear to be very good candidates for studying the situation of non-equilibrium. A most interesting point is that deep quenches of some of these phases reveal a glass transition at T_g. These systems show all the features of a conventional glass while the underlying lattice is preserved. In this so-called glassy crystal [1] family, cyanoadamantane (CNa) seems particularly promising because of the simplicity of its structure [2], the possibility of quenching single crystals [3], and a rich pattern of low-temperature (LT) non-equilibrium manifestations [4]. However, a full investigation of this system above T_g is impossible because the lifetime of metastability is too short and the transformation to the stable LT phase destroys the single crystal. Replacing the CN group by the smaller Cl substituent which gives chloroadamantane (Cla) does not lead to changes in the disordered crystalline structure [5]. However, any undercooling of Cla below the ordering phase transition is impossible. On the other hand, it has been recently reported that CNa and Cla can form a solid solution at room temperature (RT) while keeping the interesting undercooling ability over quite a wide range of concentrations [6]. An investigation of the slow structural relaxations that we are performing on these quenched compounds shows up wider perspectives than CNa [7, 8]. In this paper we present x-ray data and differential scanning calorimetry (DSC) analyses of the (CNa)$_{1-x}$(Cla)$_x$ mixed compounds with $x = 0.25$ in order to determine their equilibrium phase diagram and glass-forming conditions. Comparison with the properties of the pure compounds will be presented.

0953-8984/92/489509+08$07.50

2. Experimental details

Highly purified CNa and Cla as well as mixed compounds were crystallized by slow evaporation at RT of a slightly undersaturated solution of the products in methanol. The compositions of the mixed crystals were checked directly by inspection of the lattice parameters and subsequently by chromatography. Perfect syncrystallization appears as indicated by the sharpness of the x-ray diffraction peaks. Single-crystal x-ray experiments were performed on a four-circle diffractometer equipped with a pyrolitic graphite monochromator ($\lambda_{\mathrm{Mo\,K}\alpha} = 0.711$ Å). Powder x-ray measurements prepared by grinding single crystals were carried out using Cu Kα radiation and a curved position-sensitive detector. The Debye–Scherrer patterns were thus simultaneously recorded over a 120° range in 2θ with a 4096-channel analyser.

In both cases the LTs were achieved by setting the sample in a gaseous nitrogen flow at the required temperature. This system allows the sample to be quenched in a few seconds. Thermal measurements were performed between 100 K and RT on a DSC7 Perkin–Elmer microcalorimeter. The calibrations in temperature and energy were made using the transition points of cyclohexane and checked by measuring the C_p of sapphire.

3. Stable phases of the $(CNa)_{1-x}$ $(Cla)_x$ compounds ($x = 1$, $x = 0$ and $x = 0.25$)

We are mainly concerned with the identification of the stable phases of the mixed compound. As the growth of a single crystal of the mixed compound directly at a LT is difficult, we have attempted a powder diffraction study; this is then helped by comparison with the spectra of the pure compounds.

3.1. High-temperature disordered phases

Figures 1(*a*), 1(*b*) and 1(*c*) show the diffraction profiles for high-temperature (HT) phases for $x = 1$, $x = 0$ and $x = 0.25$, respectively, at RT. Their general outlook is the same. They are characterized by two strong peaks at small θ-values whose lattice spacings are in the $2/\sqrt{3}$ ratio, typical of the (111) and (200) reflections of the FCC lattice. The rapid decrease in intensity with increasing Bragg angle indicates that the three structures are disordered. The spectra can be indexed in the same $Fm3m$ group with the following cubic lattice parameters (table 1):

$$a_{x=0} = 9.81 \text{ Å} \qquad a_{x=1} = 9.97 \text{ Å} \qquad a_{x=0.25} = 9.83 \text{ Å}.$$

For $x = 0$ and $x = 1$ they correspond to the isomorphous orientationally disordered phases whose structures have been published previously [2, 5]. The molecular dipoles can randomly take six orientations along the ⟨100⟩ directions. For $x = 1$, the decrease in intensity with increasing θ is more rapid. This reflects the larger disorder of dipoles whose orientations are less strongly localized. This is a result of the smaller molecular volume and larger lattice parameter. The decrease in compactness in going from $x = 0$ to $x = 1$ causes a considerable decrease in dipolar residence time: $\tau_{x=0} = 8.5 \times 10^{-7}$ s and $\tau_{x=1} = 7.2 \times 10^{-13}$ s at $T = 295$ K [9, 10]. Figure 1(*c*) demonstrates that the structure of the mixed compound is isomorphous to that of the pure compounds. Furthermore, the close resemblance of the spectra of the $x = 0$ and $x = 0.25$ compounds as well as the very similar values of both their lattice

constants and residence times ($\tau_{x=0.25} = 3.0 \times 10^{-7}$ s at 295 K [11]) indicate that steric hindrance [12] is as efficient in both systems in localizing and slowing down the dipoles. It is probably this constraint which also allows the disordered phase of the mixed compound to be easily undercooled.

3.2. Stable low-temperature phases

3.2.1. Pure CNa ($x = 0$). Below 283 K the stable state is a monoclinic phase ($C2/m$) [2] (to be called II). The dipoles point in a [111] direction of the strongly distorted cubic phase and form an antiferroelectric order. The corresponding powder spectrum is shown in figure 1(*d*). It has been obtained at 205 K after aging for 10 h to assure complete conversion of the sample. The equilibrium II–I transition is measured at 283 K upon reheating.

3.2.2. Pure Cla ($x = 1$). Upon cooling, Cla transforms in its non-rotational LT phase III at 246 K. No undercooling is observed. The x-ray spectrum thus obtained is shown in figure 1(*e*). It can be indexed as monoclinic $P2_1/C$ [5]. It clearly differs from that of phase II of CNa and can be recognized by the presence of weak Bragg peaks at small angles and the splitting of the former $(111)_c$ and $(200)_c$ reflections in a group of five strong peaks in the 2θ range [15°, 20°].

3.2.3. Mixed compound ($x \neq 0.25$). Mixed compounds with concentrations up to $x \simeq 0.5$ all show easy undercooling. We mainly focused on the $x = 0.25$ value. The equilibrium phase transition at $T_t = 238$ K (see section 4 below) can only be observed upon heating and after a long LT aging. The kinetics of transformation from the metastable phase I to the LT stable phase are the most rapid for undercoolings of 20–40 K. The temporal evolution of the x-ray spectrum during the transformation has been followed to make the final indexation easier.

The progressive dropping of the cubic $(111)_c$ and $(200)_c$ reflections during aging following a quench at 218 K is shown in figure 2. In the spectrum recorded after 490 min the $(200)_c$ peak has clearly vanished. This clears up the situation around the initial position of the $(111)_c$ peak ($2\theta = 16°$) and proves that two new peaks of the LT phase have appeared. As demonstrated in figure 1(*f*), the overall LT spectrum shows all the features characteristic of phase III of Cla and will thus also be called III in the following. All the peaks can indeed be indexed as monoclinic $P2_1/c$ with parameters close to those of Cla (table 1). As for the latter a pseudo-FCC lattice can be defined (figure 3 and table 1) but it undergoes weaker deformations. In the (100) plane the shear distortion and parameter contractions with respect to the cubic cell are $\Delta\alpha = +1.4°$ and $\Delta B_c/B_c = -3.3\%$.

The dilation along the A_c axis is $\Delta A_c/A_c = 1.2\%$. This results in a volume change with respect to the metastable cubic phase taken at the same temperature which is of the order of $\Delta V/V = 2.2\%$. This should be compared with the larger 6% volume change observed at the III–I transition of Cla.

One can conclude that the dipolar order is most certainly identical with that of Cla [5], as schematically shown in figure 3. The molecular dipoles exhibit an orthogonal order inside $(100)_m$ planes. These planes form an antiferroelectric sequence along the a direction. Contrary to phase II of CNa, molecules are oriented along the former cubic $(100)_c$ directions. We could check that somewhat different values of the concentration ($0.2 < x < 0.3$) lead to the same LT spectrum; it is thus reasonable to infer a random distribution of Cla and CNa molecules. The onset of this new phase

Table 1. Summary of the structural parameters of $(CNa)_{1-x}$ $(Cla)_x$ for Cla concentrations x of 0, 0.25 and 1 at various temperatures.

Cla concentration x	Structure	T (K)	Cell parameters a (Å)	b (Å)	c (Å)	α (deg)	β (deg)	γ (deg)	Glassy crystal	Reference
0	I, FCC $Fm3m$; $T_t = 283$ K;	295	9.81	—	—	90.00	—	—	Yes; $T_g = 170$ K;	[2]
	II, monoclinic $C2/m$	240	11.28	6.87	12.10	90.00	101.30	90.00	$\dot{T} = 40$ K min^{-1}	
0.25	I, FCC $Fm3m$; $T_t = 238$ K;	295	9.83	—	—	90.00	—	—		
	pseudo-cubic III, monoclinic $P2_1/C$	205	9.95	6.82	13.27	90.00	90.19	90.00	Yes; $T_g = 163$ K;	This paper
		205	9.95	9.51	9.51	90.00	91.59	90.00	$\dot{T} = 10$ K min^{-1}	
1	I, FCC $Fm3m$; $T_t = 246$ K,	295	9.97	—	—	90.00	—	—	No	[5]
	pseudo-cubic III, monoclinic $P2_1/C$	210	10.02	6.82	13.15	90.00	90.04	90.00		
		210	10.02	9.47	9.47	90.00	92.1	90.00		

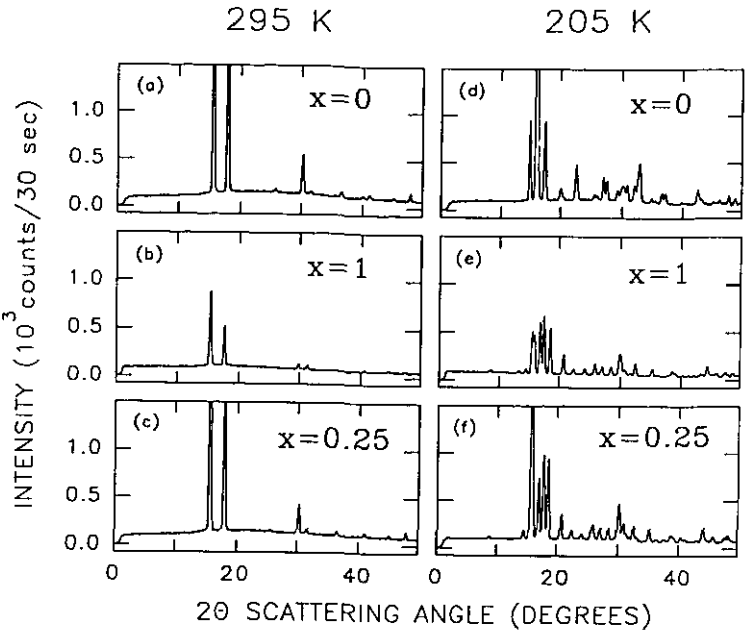

Figure 1. X-ray powder diffraction patterns of $(CNa)_{1-x}$ $(Cla)_x$ for $x = 0$, $x = 1$ and $x = 0.25$: (*a*)–(*c*) the stable HT disordered phases; (*d*)–(*f*) the stable LT ordered phases.

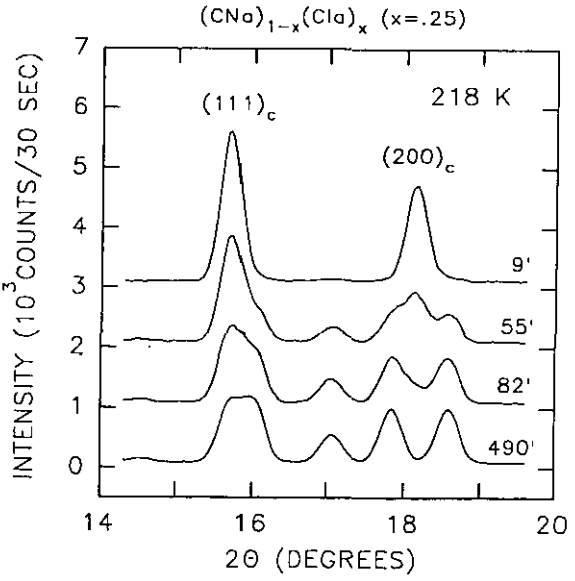

Figure 2. Temporal evolution of the x-ray powder diffraction pattern of the $(CNa)_{1-x}$ $(Cla)_x$ mixed compound ($x = 0.25$) after a quench at 218 K. The aging times are indicated on the right in the figure. The bottom pattern corresponds to the unit on the left-hand axis whereas each of the other patterns is shifted by 10^3 counts per 30 s higher than the pattern below it.

is manifested by the appearance of superstructure peaks located at the X points and $q_0 = \langle 0, 0.5, 0.5 \rangle$ points of the former cubic Brillouin zone.

4. The III–I transition and the glass transition of $(CNa)_{1-x}$ $(Cla)_x$ ($x = 0.25$)

4.1. The III–I transition

A slow temperature sweep performed after the complete transformation does not reveal any further structural phase transition between 100 and 237 K. This indicates that phase III is the stable phase in this temperature range. To characterize the III–I transition, superstructure peaks have been followed, upon heating, by single-crystal x-ray diffraction which produces a higher scattered intensity at the superstructure position. This is possible because the crystal is not destroyed during the aging which is in contrast with the situation encountered in CNa [7]. The results are shown in figure 4 for the $(300)_c$ superstructure peak. Upon isothermal aging at 213 K, the strong increase in intensity follows a 10 min induction period and saturates after 2 h. The overall growth curve is sigmoidal and can be fitted to an Avrami law $I(t) = 1 - \exp[-(t/\tau)^n]$ which is typical of a nucleation and growth process [13]. The value $n \simeq 3$ found for the exponent could indicate a preferentially two-dimensional mode of transformation. Upon heating, 10% of intensity is lost in a continuous precursor extending from 213 K to T_t. The peak then drops abruptly at $T_t = 238 \pm 1$ K and the stable FCC disordered phase is restored. One can see a residual intensity which slowly decreases for $T > T_t$. It seems to have a kinetic origin and cannot be attributed to some pre-transitional effects since this behaviour is not reversible when a new cooling is carried out. In this process the cubic phase can again be considerably undercooled below T_t.

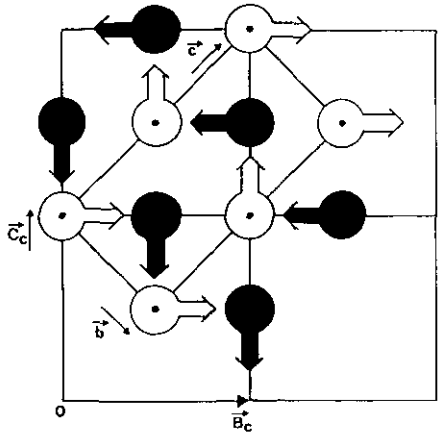

Figure 3. Mixed compounds ($x = 0.25$): dipolar orientational order in the (B_c, C_c) plane of the pseudo-cubic and monoclinic lattices of the ordered LT phase (III). Black and white dipoles, respectively, are associated with the planes $x/A_c = \frac{1}{4}$ and $x/A_c = \frac{3}{4}$. CNa and Cla molecules are randomly distributed in the lattice.

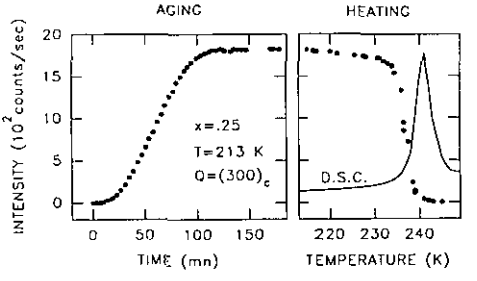

Figure 4. Time and temperature evolutions of the 300 peak intensity during aging for 3 h at 213 K and during heating from 213 K to RT ($\dot{T} = 0.5$ K min^{-1}): DSC curve measured on a Perkin–Elmer DSC 7 apparatus by heating the sample ($\dot{T} = 10$ K min^{-1}.

DSC measurements on a 17 mg sample (10 K min^{-1} heating) performed after a similar LT aging is also represented in figure 4. It shows a pronounced endothermal peak whose onset is slightly shifted above the (x-ray) T_t owing to the more rapid heating rate. The area under this sharp endotherm is about 25.8 J g^{-1}.

All these clues indicate that the III–I transition is of first order. Compared with Cla this III–I transition occurs at a somewhat lower temperature but it can be easily bypassed because dipolar residence times are very long as in phase I of CNa. However, the transition of the mixed compound sustains appreciably lower values of heat and volume discontinuities than the II–I transition of CNa itself does. This results in a decrease in the driving force for the transformation and leads to a more coherent nucleation of the LT phase. Both effects contribute to make the investigation of phase I in its metastable state easier than in the case of CNa.

4.2. The glass transition

After a quench at LT ($\dot{T} \simeq 50$ K s^{-1}; $T \leqslant 140$ K), one gets a stationary x-ray spectrum which is fully similar to that recorded at RT and does not provide any evidence of transformation towards the LT phase. This proves that the underlying FCC lattice and consequently the orientational disorder are preserved. To display a possible macroscopic glass transition, DSC measurements were performed with a 44 mg sample previously chilled at 103 K with a cooling rate of -200 K min^{-1} from RT. Figure 5 shows the heating curve $C_p(T)$ with the rate of $+10$ K min^{-1}. Under this condition no trace of exothermic transformation is seen and no endothermal accident occurs at 238 K. One observes a pronounced heat capacity jump which signals a glass transition at $T_g \simeq 163$ K. The ratio of the C_p-values taken respectively above and below T_g: $[C_p(\text{disorder})/C_p(\text{glass})]_{T_g} \simeq 1.4$ is noticeably higher than 1.1 which is considered to be a typical value for a so-called strong glass [14]. As for CNa, deep undercooling thus leads to a glassy crystal state which can be ascribed to the freezing of the slowest molecular rotations (i.e. dipolar tumbling). In CNa the extrapolated residence time of the dipolar tumbling is about 500 s at 170 K which is the calorimetric glass transition of this compound [15]. For the same temperature scanning rate the value of T_g found for the mixed compound is somewhat lower (cf table 1). This is a consequence of the slightly shorter time scale of the dipolar dynamics in this latter case.

While the mixed compound exhibits a glass transition and a glassy crystalline state with characteristics similar to those of CNa, it appears to be a better glass former. As shown in figure 4 the time to escape from the metastable state in the temperature range of most rapid transformation is of the order of a tens of minutes. Furthermore a single crystal is not completely destroyed by the transformation so that interesting information can still be obtained during and after the transformation. A similar investigation with CNa would have led to a much more rapid and complete destruction of the single crystal. These two behaviours must be ascribed to the different relations existing between the HT and LT lattices for each compound.

Advantage has been taken of the easier investigation of the metastable state in [7] from which figure 5 is taken. Measurements of lattice parameters could be performed both below and above T_g. They show a pronounced jump in the thermal expansion coefficient α, parallel to that of C_p at the glass transition. This provides experimental evidence that the freezing mechanism must certainly involve both the slowing down of the orientational ordering and a structural relaxation process. This is probably a

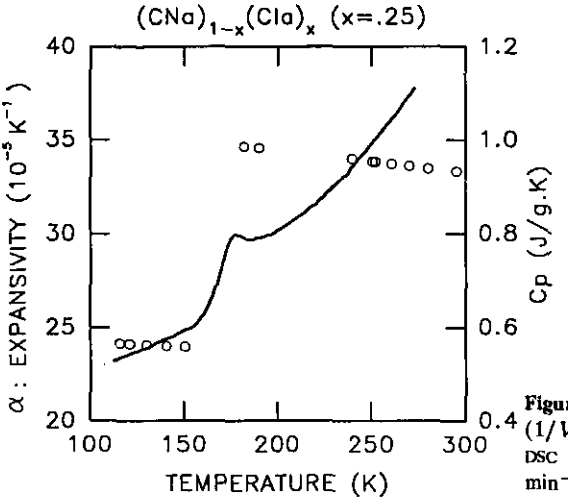

Figure 5. Thermal expansion coefficient $\alpha = (1/V)\ (\partial V/\partial T)$ versus temperature (○) and the DSC curve obtained upon heating ($\dot{T}$ = 10 K min^{-1}) (——).

crucial point that needs to be examined in order to clarify the mechanism of the glass transition in glassy crystals.

Acknowledgment

This work was supported by the EC Science contract SC1-0426-C (CD).

References

[1] Suga H and Seki S 1974 *J. Non-Cryst. Solids* **16** 171
[2] Foulon M, Amoureux J P, Sauvajol J L, Cavrot J P and Muller M 1984 *J. Phys. C: Solid State Phys.* **17** 4213
[3] Foulon M, Amoureux J P, Sauvajol J L, Lefebvre J and Descamps M 1983 *J. Phys. C: Solid State Phys.* **16** L265
[4] Descamps M and Caucheteux C 1987 *J. Phys. C: Solid State Phys.* **20** 5073
[5] Foulon M, Belgrand T, Gors C and More M 1989 *Acta Crystallogr.* B **45** 404
[6] Foulon M 1987 *Thèse d'état* University of Lille I
[7] Descamps M, Willart J F, Odou G and Eichhorn K 1992 *J. Physique* I **6** 813–27
[8] Willart J F 1991 *Thesis* University of Lille I
[9] Amoureux J P, Noyel G, Foulon M, Bee M and Jorat L 1984 *Mol. Phys.* **52** 161
[10] Bee M and Amoureux J P 1983 *Mol. Phys.* **48** 68
[11] Descamps M, Willart J F, Legrand C and Obrihaye O 1992 to be published
[12] Descamps M 1982 *J. Phys. C: Solid State Phys.* **15** 7265
[13] Axe J D and Yamada Y 1986 *Phys. Rev.* B **34** 1599
[14] Angell C A 1991 *J. Non-Cryst. Solids* **131–33** 13
[15] Pathmanathan K and Johari G P 1985 *J. Phys. C: Solid State Phys.* **18** 6535